

A Dispersive Analysis on the $f_0(600)$ and $f_0(980)$ Resonances in $\gamma\gamma \rightarrow \pi^+\pi^-, \pi^0\pi^0$ Processes

YU MAO,¹ XUAN-GONG WANG,¹ OU ZHANG,¹ H. Q. ZHENG,¹
Z. Y. ZHOU²

1: Department of Physics, Peking University, Beijing 100871, China

2: Department of Physics, Southeast University, Nanjing 211189, China

November 7, 2018

Abstract

We estimate the di-photon coupling of $f_0(600)$, $f_0(980)$ and $f_2(1270)$ resonances in a coupled channel dispersive approach. The $f_0(600)$ di-photon coupling is also reinvestigated using a single channel T matrix for $\pi\pi$ scattering with better analyticity property, and it is found to be significantly smaller than that of a $\bar{q}q$ state. Especially we also estimate the di-photon coupling of the third sheet pole located near $\bar{K}K$ threshold, denoted as $f_0^{III}(980)$. It is argued that this third sheet pole may be originated from a coupled channel Breit-Wigner description of the $f_0(980)$ resonance.

PACS: 11.55.Fv; 11.80.Et; 13.40.-f; 13.75.Lb

1 Introduction

The study on the $\gamma\gamma \rightarrow \pi\pi$ process has received renewed interests recently on both experimental [1] and theoretical side. [2] One major motivation to drive the studies on the process is to extract the two photon coupling of the resonant states appearing in the reaction, which is helpful in exploring the underlying structure of these (often weird) states, as emphasized by Pennington. [3] An incomplete list of theoretical studies along this line may be found in Refs. [4] – [12].

In this paper we will also devote to the study on the $\gamma\gamma \rightarrow \pi^+\pi^-, \pi^0\pi^0$ processes. We proceed with previous calculations, but now take into account the coupled channel effects in the most interesting $IJ = 00$ channel. Section 2 reviews the coupled channel formalism needed in this study, including: spectral function representation, analytic continuation of coupled channel $\gamma\gamma$ scattering amplitudes, and the dispersive integral representation of the latter. In section 3 we review the basic technique of partial wave expansion and how to estimate the Born term contributions. In section 4 we devote to a redetermination to the coupled channel $\pi\pi, \bar{K}K$ scattering T matrices previously proposed, [13]

with the help of new experimental inputs at very low energies. [14] Section 5 is devoted to the numerical analysis on the $\gamma\gamma \rightarrow \pi^+\pi^-, \pi^0\pi^0$ processes, both in coupled channel and in single channel formalism. Finally in section 6 we draw conclusions based on the numerical studies.

2 Couple channel formalism for the $\gamma\gamma \rightarrow \pi\pi, \bar{K}K$ processes

2.1 Spectral function representations

In the coupled channel case the relation between (the 2 by 2) S matrix and T matrix is

$$S = 1 + 2i\rho^{1/2}T\rho^{1/2}, \quad (1)$$

where $\rho = \text{diag}(\rho_1, \rho_2)$ and $\rho_n = \sqrt{1 - 4m_n^2/s}$. Here subscripts $n = 1, 2$ represent $\pi\pi, \bar{K}K$ channels, respectively.

Let F_1, F_2 be the $\gamma\gamma \rightarrow \pi\pi, \bar{K}K$ amplitudes, respectively, $F \equiv (F_1, F_2)^T$. Define $F^\pm(s) = \lim_{\epsilon \rightarrow 0^+} F(s \pm i\epsilon)$, then F obeys the following spectral representation in the physical region:

$$\begin{aligned} \text{Im}F_1 &= F_1\rho_1T_{11}^* + F_2\rho_2T_{12}^*, \\ \text{Im}F_2 &= F_1\rho_1T_{21}^* + F_2\rho_2T_{22}^* \end{aligned} \quad (2)$$

above $\bar{K}K$ threshold and

$$\begin{aligned} \text{Im}F_1 &= F_1\rho_1T_{11}^*, \\ \text{Im}F_2 &= F_1\rho_1T_{21}^* \end{aligned} \quad (3)$$

when s lies between first and second threshold. From Eqs. (2), (3), along positive real axis, one has a shorthand expression,

$$F^+ = \begin{pmatrix} F_1^+ \\ F_2^+ \end{pmatrix} = \tilde{S}F^- \equiv \begin{pmatrix} 1 + 2i\rho_1T_{11}\theta_1 & 2i\rho_2T_{12}\theta_2 \\ 2i\rho_1T_{21}\theta_1 & 1 + 2i\rho_2T_{22}\theta_2 \end{pmatrix} \begin{pmatrix} F_1^- \\ F_2^- \end{pmatrix} \quad (4)$$

where $\theta_1 = \theta(s - 4m_\pi^2)$ and $\theta_2 = \theta(s - 4m_K^2)$ are step functions.

From above spectral function representations, the analytic continuation of F to different sheets can be obtained:

$$\begin{aligned} F^{II} &= B_{II}F \equiv \begin{pmatrix} \frac{1}{1+2i\rho_1T_{11}^I}, & 0 \\ \frac{-2i\rho_1T_{12}^I}{1+2i\rho_1T_{11}^I}, & 1 \end{pmatrix} F, \\ F^{III} &= B_{III}F \equiv \begin{pmatrix} \frac{1+2i\rho_2T_{22}^I}{\det S}, & \frac{-2i\rho_2T_{21}^I}{\det S} \\ \frac{-2i\rho_1T_{12}^I}{\det S}, & \frac{1+2i\rho_1T_{11}^I}{\det S} \end{pmatrix} F, \\ F^{IV} &= B_{IV}F \equiv \begin{pmatrix} 1, & \frac{-2i\rho_2T_{21}^I}{1+2i\rho_2T_{22}^I} \\ 0, & \frac{1}{1+2i\rho_2T_{22}^I} \end{pmatrix} F. \end{aligned} \quad (5)$$

These expressions of analytic continuation will be used later when extracting the residue couplings of each resonance.

2.2 Dispersive representation for $\gamma\gamma \longrightarrow \pi\pi, \bar{K}K$ amplitudes

In this subsection we review the method originally proposed by Basdevant and collaborators [5] on how to set up the dispersive representation for the $\gamma\gamma \rightarrow \pi\pi$ amplitudes.

On the right hand cut, $F^+ = \tilde{S}F^-$. Further let $\tilde{F} = F - F_L$, F_L contains only left hand cut of F . In this paper we approximate F_L by its Born term, F_B . Then on the positive real axis one has,

$$F = \tilde{F} + F_B , \quad (6)$$

$$F^+ = (\tilde{F} + F_B)^+ = \tilde{F}^+ + F_B = \tilde{S}F^- = \tilde{S}(\tilde{F}^- + F_B) , \quad (7)$$

$$\tilde{F}^+ = \tilde{S}\tilde{F}^- + (\tilde{S} - 1)F_B . \quad (8)$$

Next we will search for a 2×2 invertible matrix function $D(s)$, which is analytic on the cut s plane and only contains right hand cut (*r.h.c.*), and on the *r.h.c.* it obeys the same unitarity equation as $F(s)$. That is

$$D^+(s) = \tilde{S}(s)D^-(s) , \quad \text{or} \quad \tilde{S} = D^+(D^-)^{-1} . \quad (9)$$

One can then deduce from the above equation and Eq. (8) that

$$\text{Im}D^{-1}\tilde{F} = -\text{Im}D^{-1}F_B , \quad (10)$$

from which one obtains a dispersive representation for \tilde{F}^+

$$\tilde{F}^+ = -\frac{D^+}{\pi} \int_{s_0}^{\infty} \frac{\text{Im}D^{-1}F_B}{s' - s - i\epsilon} ds' + D^+P , \quad (11)$$

where P is a 2 dimensional array of subtraction polynomial, and a proper subtraction is understood on the dispersion integral. By making use of Low's theorem [16] which tells that when $s \rightarrow 0$, $F(s) \rightarrow F_B(s)$, we can rewrite the above equation with one more subtraction, and obtain: [17]

$$F(s) = F_B + D(s)[Ps - \frac{s^2}{\pi} \int_{4m_\pi^2}^{\infty} \frac{\text{Im}D^{-1}(s')F_B(s')}{s'^2(s' - s - i\epsilon)} ds'] . \quad (12)$$

From the above discussion we know that the $\gamma\gamma \rightarrow \pi\pi, \bar{K}K$ amplitudes can be fit with parameter(s) P , once $D(s)$ and $F_B(s)$ are known.

2.3 Solution of function $D(s)$

The 2 by 2 matrix function $D(s)$ only contains right hand cuts, and satisfies the similar unitarity relations as F :

$$\begin{aligned} \text{Im}D_{11} &= D_{11}\rho_1 T_{11}^* \theta_1 + D_{21}\rho_2 T_{12}^* \theta_2 , \\ \text{Im}D_{21} &= D_{11}\rho_1 T_{21}^* \theta_1 + D_{21}\rho_2 T_{22}^* \theta_2 ; \end{aligned} \quad (13)$$

$$\begin{aligned}\text{Im}D_{21} &= D_{12}\rho_1 T_{11}^* \theta_1 + D_{22}\rho_2 T_{12}^* \theta_2 , \\ \text{Im}D_{22} &= D_{12}\rho_1 T_{21}^* \theta_1 + D_{22}\rho_2 T_{22}^* \theta_2 .\end{aligned}\tag{14}$$

The above two equations have the same structure as the following

$$\begin{aligned}\text{Im}\chi_1 &= \chi_1 \rho_1 T_{11}^* \theta_1 + \chi_2 \rho_2 T_{12}^* \theta_2 , \\ \text{Im}\chi_2 &= \chi_1 \rho_1 T_{21}^* \theta_1 + \chi_2 \rho_2 T_{22}^* \theta_2 .\end{aligned}\tag{15}$$

Hence searching for solutions of $D(s)$ is equivalent to searching for two independent solutions of the equation for the two dimensional array $(\chi_1, \chi_2)^T$. The two independent solutions can be identified as $(D_{11}, D_{21})^T$ and $(D_{12}, D_{22})^T$. The integral equation to solve Eq. (15) is

$$\begin{aligned}\chi_1^{(N+1)}(s) &= \chi_1(0) + \frac{s}{\pi} \int_{4m_\pi^2}^{\Lambda^2} \frac{\text{Re}[\chi_1^N(s') \rho_1(s') T_{11}^*(s') \theta_1]}{s'(s' - s - i\epsilon)} ds' \\ &\quad + \frac{s}{\pi} \int_{4m_\pi^2}^{\Lambda^2} \frac{\text{Re}[\chi_2^N(s') \rho_2(s') T_{12}^*(s') \theta_2]}{s'(s' - s - i\epsilon)} ds' , \\ \chi_2^{(N+1)}(s) &= \chi_2(0) + \frac{s}{\pi} \int_{4m_\pi^2}^{\Lambda^2} \frac{\text{Re}[\chi_1^N(s') \rho_1(s') T_{21}^*(s') \theta_1]}{s'(s' - s - i\epsilon)} ds' \\ &\quad + \frac{s}{\pi} \int_{4m_\pi^2}^{\Lambda^2} \frac{\text{Re}[\chi_2^N(s') \rho_2(s') T_{22}^*(s') \theta_2]}{s'(s' - s - i\epsilon)} ds' ,\end{aligned}\tag{16}$$

where N denotes the number of steps in the iteration, the integration is truncated at $\Lambda^2 = 2.4\text{GeV}^2$. On the *r.h.s.* of above equation, we take the real part of the numerator in the integrand which is of great help in increasing the speed of convergence. [18] In the numerical calculation a convergent solution emerges after approximately 15 steps of iteration.

In this paper we solve the coupled channel $D(s)$ function in the case of $I, J = 0, 0$, for a given T matrix. For the two d waves and the $I = 2$ s wave we only use single channel approximation, and in such simplified case the solution to the function $D(s)$ is known as the Omnés solution,

$$D(s) = \exp \left(\frac{s}{\pi} \int_{4m_\pi^2}^{\infty} \frac{\delta(s') ds'}{(s' - s)s'} \right) .\tag{17}$$

2.4 Analytic continuation, pole residues and $\Gamma(f \rightarrow \gamma\gamma)$

In order to extract pole residues on different sheets a knowledge of analytic continuation to the complex plane is needed. Firstly, the analytic continuation of function $D(s)$ is simple. It satisfies the following dispersive integral equation

$$D(s) = D(0) + \frac{s}{\pi} \int_{4m_\pi^2}^{\infty} \frac{D(s') \rho(s') T^*(s') \theta}{s'(s' - s)} ds' .\tag{18}$$

$D(s), \rho(s), T(s), \theta$ in above can all be matrix functions in above formula. To calculate D with complex argument z on the first Riemann sheet one only

needs to replace $s \rightarrow z$ in above integral formula. For function F the analytic continuation is more involved, in the following we discuss this topic in some details.

Residues of second sheet poles:

Since in the vicinity of a pole z_{II} , $S(s \sim z_{II}) \simeq S'(z_{II})(s - z_{II})$ and

$$T^{II}(\pi\pi \rightarrow \pi\pi)(s \rightarrow z_{II}) = \frac{T^I(s \rightarrow z_{II})}{S'(z_{II})(s - z_{II})} \quad (19)$$

$$F^{II}(\gamma\gamma \rightarrow \pi\pi)(s \rightarrow z_{II}) = \frac{F^I(s \rightarrow z_{II})}{S'(z_{II})(s - z_{II})} \quad (20)$$

and through the definition of coupling constants:

$$\begin{aligned} T(\pi\pi \rightarrow \pi\pi)(s \rightarrow z_R) &= \frac{g_\pi^2}{z_R - s}, \\ F(\gamma\gamma \rightarrow \pi\pi)(s \rightarrow z_R) &= \frac{g_\gamma g_\pi}{z_R - s}, \end{aligned} \quad (21)$$

one obtains the expressions of g_π and g_γ for second sheet poles:

$$g_\pi^2 = -\frac{T(z_{II})}{S'(z_{II})}, \quad g_\gamma g_\pi = -\frac{F(z_{II})}{S'(z_{II})}. \quad (22)$$

Residues of third sheet poles:

Denote the third sheet pole as z_{III} , which is the zero of $\det S$, then

$$\det S(s \rightarrow z_{III}) = (\det S)'(z_{III})(z - z_{III}). \quad (23)$$

From

$$T^{III} = T^I B^{III} = \begin{pmatrix} T_{11} & T_{12} \\ T_{21} & T_{22} \end{pmatrix} \begin{pmatrix} \frac{1+2i\rho_2 T_{22}}{\det S} & \frac{-2i\rho_1 T_{21}}{\det S} \\ \frac{-2i\rho_2 T_{12}}{\det S} & \frac{1+2i\rho_1 T_{11}}{\det S} \end{pmatrix}, \quad (24)$$

the residues are hence obtainable, according to Eq. (21):

$$g_\pi^2 = \frac{S_{22}(z_{III})}{2i\rho_1 \det S'(z_{III})}, \quad g_K^2 = \frac{S_{11}(z_{III})}{2i\rho_2 \det S'(z_{III})}. \quad (25)$$

From Eq. (5) one further gets

$$g_\gamma g_\pi = -\frac{F_1^I(z_{III})S_{22}(z_{III})}{(\det S)'(z_{III})} + \frac{F_2^I(z_{III})2i\rho_2(z_{III})T_{21}^I(z_{III})}{(\det S)'(z_{III})}, \quad (26)$$

$$g_\gamma g_K = \frac{F_1^I(z_{III})2i\rho_1(z_{III})T_{12}^I(z_{III})}{(\det S)'(z_{III})} - \frac{F_2^I(z_{III})S_{11}(z_{III})}{(\det S)'(z_{III})}. \quad (27)$$

Having obtained the two photon couplings, g_γ , the width of σ , $f_0(980)$ and $f_2(1270)$ to two photons can be calculated,

$$\Gamma_{\gamma\gamma}^R(pole) = \frac{\alpha^2 \beta_R |g_\gamma|^2}{4(2J+1)m_R}. \quad (28)$$

where $\alpha = 1/137$ is the fine structure constant and $\beta_R = (1 - 4m_\pi^2/m_R^2)^{1/2}$.

3 Partial Waves and the Born term contributions

3.1 Partial wave expansions

For the $\gamma\gamma \rightarrow \pi\pi$ process there are two independent helicity amplitudes M_{++} , M_{+-} . The former corresponds to photon helicity difference $\lambda = 0$ the latter corresponds to $\lambda = 2$. They contribute to the differential cross-section as: [4]

$$\frac{d\sigma}{d\Omega} = \frac{\rho}{128\pi^2 s} [|M_{++}|^2 + |M_{+-}|^2] , \quad (29)$$

where $\rho = [1 - 4m_\pi^2/s]^{1/2}$, and they have partial wave expansions involving only even $J(\geq \lambda)$,

$$M_{++}(s, \theta, \phi) = e^2 \sqrt{16\pi} \sum_{J \geq 0} F_{J0}(s) Y_{J0}(\theta, \phi) , \quad (30)$$

$$M_{+-}(s, \theta, \phi) = e^2 \sqrt{16\pi} \sum_{J \geq 2} F_{J2}(s) Y_{J2}(\theta, \phi) . \quad (31)$$

With this normalization the total cross-section reads,

$$\sigma = 2\pi\alpha^2 \frac{\rho}{s} \sum_{J \geq \lambda} |F_{J\lambda}|^2 . \quad (32)$$

At very low energies the major contribution to the amplitudes comes from one π exchange (OPE), i.e., the Born term, as guaranteed by Low's theorem. [16]

$$M_{+\pm}(s, t) \rightarrow M_{+\pm}^B(s, t), \quad (s \rightarrow 0, t \rightarrow m_\pi^2) . \quad (33)$$

Denoting s -channel partial wave of the Born amplitude as $B_{J\lambda}(s)$, then Low's theorem implies

$$\frac{F_{J\lambda}(s)}{B_{J\lambda}(s)} \rightarrow 1, \quad F_{J\lambda}(s) - B_{J\lambda}(s) \rightarrow O(s) . \quad (34)$$

The OPE Born term amplitude for $\gamma\gamma \rightarrow \pi^0\pi^0$ vanishes and for $\gamma\gamma \rightarrow \pi^+\pi^-$ processes read,

$$M_{++}^B = M_{--}^B = 2e^2 m^2 \left(\frac{1}{m^2 - t} + \frac{1}{m^2 - u} \right) , \quad (35)$$

$$M_{+-}^B = M_{-+}^B = -\frac{2e^2(m^4 - tu)}{s} \left(\frac{1}{m^2 - t} + \frac{1}{m^2 - u} \right) , \quad (36)$$

from which OPE partial wave amplitudes are obtained: [4]

$$B_{00}(s) = \frac{1 - \rho^2}{2\rho} \ln\left(\frac{1 + \rho}{1 - \rho}\right) , \quad (37)$$

$$B_{20}(s) = \sqrt{\frac{5}{16}} \frac{(1 - \rho^2)}{\rho^2} \left[\frac{(3 - \rho^2)}{\rho} \ln\left(\frac{1 + \rho}{1 - \rho}\right) - 6 \right] , \quad (38)$$

$$B_{22}(s) = \sqrt{\frac{15}{32}} \left[\frac{(1 - \rho^2)^2}{\rho^3} \ln\left(\frac{1 + \rho}{1 - \rho}\right) + \frac{10}{3} - \frac{2}{\rho^2} \right] . \quad (39)$$

At higher energies, however, OPE Born term amplitudes are not satisfactory to describe the left cut well. One may try to improve this by adding crossed channel vector and axial vector meson exchange diagrams. Nevertheless it is difficult to judge to what extent adding vector and axial vector exchange contributions improve the situation. Further discussions will be made in section 5.1.

4 The coupled channel scattering T matrices

It is necessary to choose an appropriate T matrix in each channel. For the $I=2$ s -wave we use the result of Ref. [19]. For the $I=0$ d -wave amplitude we use the result from Ref. [20]. In both these two cases we use single channel approximation.

For the $I=0$ s -wave $\pi\pi$, $\bar{K}K$ system, to solve the matrix function $D(s)$ by iteration, a general coupled channel T matrix is required as an input. We choose the K -matrix parametrization proposed in Ref. [13] (the K_3 form) to refit low-energy $\pi\pi$ scattering data with totally 22 free parameters. The data sets we use are the phase shift and inelasticity of $I = 0$ s -wave $\pi\pi$ scattering from CERN-Munich [21] and especially from the K_{e4} experiment [14],¹ and $\phi_{12} = \delta_\pi + \delta_K$ of $\pi\pi \rightarrow K\bar{K}$ $I = 0$ s -wave scattering from several groups. [22, 23, 24, 25, 26] We have total 171 data points below 1.89GeV in the region of our interest. It is worthy mentioning that we can get an acceptable fit with a $\chi^2_{d.o.f}$ of 1.14, even including the conflicting data of ϕ_{12} from Cohen et al. and Etkin et al., but the exercise leaving aside either of them favors Etkin et al. over Cohen et al. with a $\chi^2_{d.o.f}$ of 0.68 compared with 0.99. The final fit excluding the data from Cohen et al. are shown in figure 1 and figure 2. The obtained K -matrix parameters are listed in table 1.

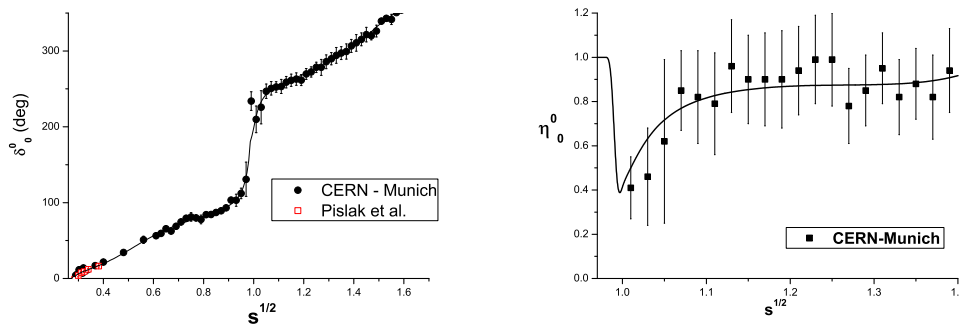


Figure 1: The fit curve of $\pi\pi$ $I = 0$ S -wave phase shift and inelasticity with CERN-Munich data [21] and data from Pislak et al. [14].

¹Adding the data from Ref. [14] is already good enough to constrain the T matrix near threshold so the most recent NA48/2 K_{e4} data is not included. [15]

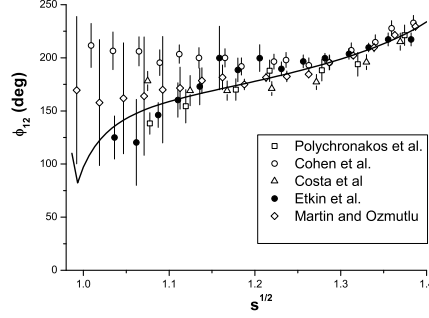


Figure 2: The phase shift $\phi_{12} = \delta_\pi + \delta_K$ of $\pi\pi \rightarrow K\bar{K}$ $I = 0$ s -wave scattering with data sets from Res. [22, 23, 24, 25, 26]. Notice that Ref. [22] is not used in the fit.

$s_0 = 0.081$	$c_{11}^0 = 7.599$	$c_{21}^0 = 15.49$
$s_1 = 0.305$	$c_{11}^1 = -16.30$	$c_{21}^1 = -15.60$
$s_2 = 0.984$	$c_{11}^2 = 7.530$	$c_{21}^2 = 17.58$
$s_3 = 3.587$	$c_{11}^3 = -2.796$	$c_{21}^3 = -4.942$
$f_1^1 = 1.499$	$c_{11}^4 = 0.0$	$c_{21}^4 = 0.0$
$f_1^2 = 1.041$	$c_{12}^0 = 15.49$	$c_{22}^0 = -6.441$
$f_2^1 = 0.089$	$c_{12}^1 = -15.60$	$c_{22}^1 = -13.53$
$f_2^2 = 0.484$	$c_{12}^2 = 17.58$	$c_{22}^2 = 31.04$
$f_3^1 = -7.714$	$c_{12}^3 = -4.942$	$c_{22}^3 = -6.830$
$f_3^2 = 9.216$	$c_{12}^4 = 0.0$	$c_{22}^4 = 0.0$

Table 1: K_3 matrix parameters obtained from the fit as described in this section. For the definition of these parameters we refer to the original paper Ref. [13].

The fit to the K_3 amplitude produces several S-matrix poles either on the second Riemann sheet or third-sheet. Those that are relevant to the current interest are listed in table 2. There we also list a third sheet pole located at $0.705 - 0.327i$, which might be considered as the third sheet counterpart of $f_0(600)$. Since it is too far away from physical region, we will not discuss it any further. The fit with a K_3 parametrization returns another pole on the third sheet, denoted as $f_0^{\text{III}}(980)$ herewith. It is of course a (K_3) model dependent prediction. This third sheet pole is close to but below $\bar{K}K$ threshold, and may be correlated to $f_0^{\text{II}}(980)$, [13, 27, 28] since the data are better described when including such a pole.² We will further discuss physics related to this pole in some detail in section 5.3.

²It is worthy emphasizing that the third-sheet pole near $K\bar{K}$ threshold moves away and disappears, if the data of Cohen et al. are taken into account.

pole	sheet-II	sheet-III
σ	$0.549 - 0.230i$	$0.705 - 0.327i$
$f_0(980)$	$0.999 - 0.021i$	$0.977 - 0.060i$

Table 2: The poles's location on the \sqrt{s} -plane, in units of GeV.

pole position	$g_{\pi\pi}^2$	g_{KK}^2
$\sqrt{s_{II}} = 0.999 - 0.021i$	$-0.07 - 0.01i$	$-0.10 + 0.09i$
$\sqrt{s_{III}} = 0.977 - 0.060i$	$-0.10 + 0.02i$	$-0.02 - 0.09i$

Table 3: $f_0(980)$ pole positions and their residues.

The σ^{II} pole is not very satisfactory comparing with the determination of Ref. [19], since a coupled channel $\pi\pi, \bar{K}K$ scattering amplitude fully compatible with analyticity and crossing symmetry is still un-available. In section 5.2 we will try to remedy this shortcoming by making use of the single channel T matrix of Ref. [19]. The pole position is not very satisfactory, and the coupling strength extracted,

$$g_{\sigma\pi\pi}^2 = (-0.07 - 0.17i)\text{GeV}^2, \quad (40)$$

differs from that given in Eq. (43) in section 5.2, though the magnitude is compatible. On the other side it is expected that the information one extracts from the coupled channel is reliable in the vicinity of $\bar{K}K$ threshold, especially for the $f_0(980)$ resonance. Couplings to $\pi\pi$ and $\bar{K}K$ of poles near $\bar{K}K$ threshold are also obtained as listed in table 3. It will be useful in section 5.3 when discussing the properties of $f_0(980)$.

5 Numerical fit to $\gamma\gamma \longrightarrow \pi^+\pi^-, \pi^0\pi^0$ process

5.1 The coupled channel fit

Only I,J=0,0 channel are calculated by solving coupled channel integral equations. Other channels are all approximated by Omnés solutions. Subtraction polynomial (constant) in different channels are listed below:

- $I, J, \lambda = 0, 0, 0$: Solve couple-channel integral equation for D and fit parameters are P_1 and P_2 .
- $I, J, \lambda = 2, 0, 0$: Use Omnés solution, the fit parameter is P_3 .
- $I, J, \lambda = 0, 2, 2$: Use Omnés function and fit P_4 .
- $I, J, \lambda = 2, 2, 2$: Since this channel's contribution is very weak, we use Born term approximation.
- $I, J, \lambda = 0, 2, 0$: Use Omnés solution and the fit parameter is P_5 .

- $I, J, \lambda = 2, 2, 0$: Since this channel's contribution is very weak, we use Born term approximation.

Here five subtraction constants are involved. Furthermore we introduce two additional form-factors to suppress the bad high energy behavior of the Born term amplitudes:

$$B_s \rightarrow B_s e^{-s/\Lambda_s^2}, \quad B_d \rightarrow B_d e^{-s/\Lambda_d^2}, \quad (41)$$

hence totally we have 7 fit parameters.

For $\gamma\gamma \rightarrow \pi^+\pi^-$ process there exist three sets of data, which are from Belle, [1] CELLO, [29] and Mark-II. [30] In our fit from $\pi^+\pi^-$ threshold to 0.9GeV, we use the Mark-II data, from 0.9GeV to 1.4GeV we use Belle data. For $\gamma\gamma \rightarrow \pi^0\pi^0$ there exist two data sets from Crystal Ball Collaboration, Refs. [31] and [32]. Here we chose the data from Ref. [31], from $\pi\pi$ threshold up to 1.4GeV.

Firstly a comparison between the contribution from OPE Born term amplitude and the contribution adding vector and axial vector meson exchanges in each channel is made, having obtained the two cutoff parameters which used to readjust the Born term amplitudes: $\Lambda_s = 1.77\text{GeV}$ and $\Lambda_d = 0.86\text{GeV}$. However it is difficult to judge whether adding vector meson and axial vector meson exchange contributions improves the OPE contribution or not, comparing with the fit results shown in figure 3, where contributions from one π exchange, vector meson exchange, axial-vector meson exchange, with corrections from the exponential form-factors (the latter are determined from the fit), are combined together and plotted. For the expressions of vector and axial vector meson exchange contributions we refer to the appendix.

The ratio between $IJ\lambda = 020$ wave and $IJ\lambda = 022$ wave may not be very stable. Though it is understood that the former should be much smaller than the latter. [33] We however find a convergent solution with $\sigma_{d0}/\sigma_{tot} \simeq 0.14$ and $\sigma_s/\sigma_{tot} \simeq 0.07$ (at the $f_2(1270)$ pole position). The first ratio given here is rather close to the ‘*dip*’ solution of Ref. [34]. The second ratio is significantly smaller than both the ‘*peak*’ and the ‘*dip*’ solution of Ref. [34]. The fit results are listed in table 4 and plotted in figure 4. The fit result on each partial wave amplitude is found to be rather similar in general with the solution B of Ref. [2] and to figure 1 of Ref. [9]. The di-photon width $\Gamma(f_2 \rightarrow 2\gamma) = 4.36\text{keV}$ here, which is larger than the value given by the solution B of Ref. [2]: $\Gamma(f_2 \rightarrow 2\gamma) = 3.82 \pm 0.30\text{keV}$. Part of the reason for such a difference may be due to the fact that the s -wave contribution given in this paper at the $f_2(1270)$ peak is smaller than that given in Ref. [2]. Also the interference between s wave and d wave is found to be destructive.³ That the result of Ref. [2] on $f_2(1270)$ di-photon width is significantly larger than the value as quoted by PDG is explained in Ref. [2] – because the Belle data gives a larger enhancement at $f_2(1270)$ peak than the previous data.

³Due to the limitation of experimental detection, the integration range of $\cos\theta$ is not from -1 to +1, hence causing a nonvanishing interference between different partial waves.

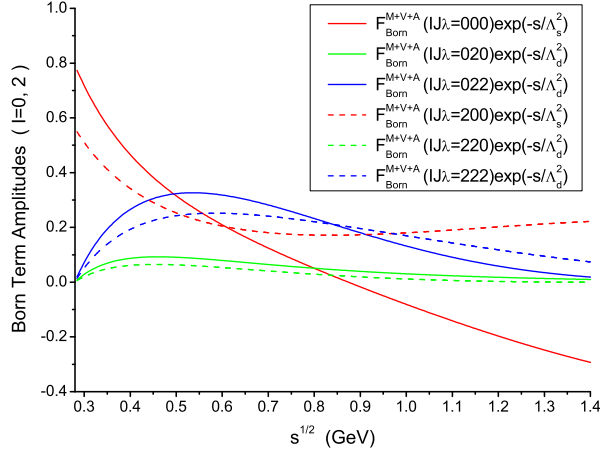


Figure 3: Born term amplitudes with corrections from exponential form factors taken into account. The parameter of form-factors are determined from the fit made in section 5.1.

	Pole-positions(GeV)	$\Gamma(f_J \rightarrow \gamma\gamma)(\text{keV})$
$f_0^{II}(980)$	$0.999 - 0.021i$	0.12
$f_0^{III}(980)$	$0.977 - 0.060i$	0.35
$f_0(600)$	$0.549 - 0.230i$	0.76
$f_2(1270)(\lambda = 0)$	$1.272 - 0.087i$	0.66
$f_2(1270)(\lambda = 2)$		3.70

Table 4: $\chi_{d.o.f}^2 = 0.5$, using T matrices as depicted in section 2.3. The central value of other 5 parameters are: $P_1 = 0.25$, $P_2 = 0.25$, $P_3 = -0.23$, $P_4 = 0.22$, $P_5 = 0.55$.

To summarize, we have the following observations through our fit:

1. It is known that the $\lambda = 2$ amplitude should dominate the $\gamma\gamma$ width of the tensor state. Even though the ratio between the $\lambda = 0$ and the $\lambda = 2$ partial wave may not be stable, a solution with a small ratio σ_{d0}/σ_{tot} is found. The total di-photon decay width of $f_2(1270)$ is however found to be rather large comparing with the value quoted by PDG and the value given in Ref. [2].
2. The $f_0(980) \rightarrow \gamma\gamma$ width is found to be very small. It is in agreement with the solution B in Ref. [2]. See table 6 for a comparison between different model predictions.
3. We also give the $f_0^{III}(980)$ width to two photons, which is not seen in previous literature. However the third sheet pole's position and hence

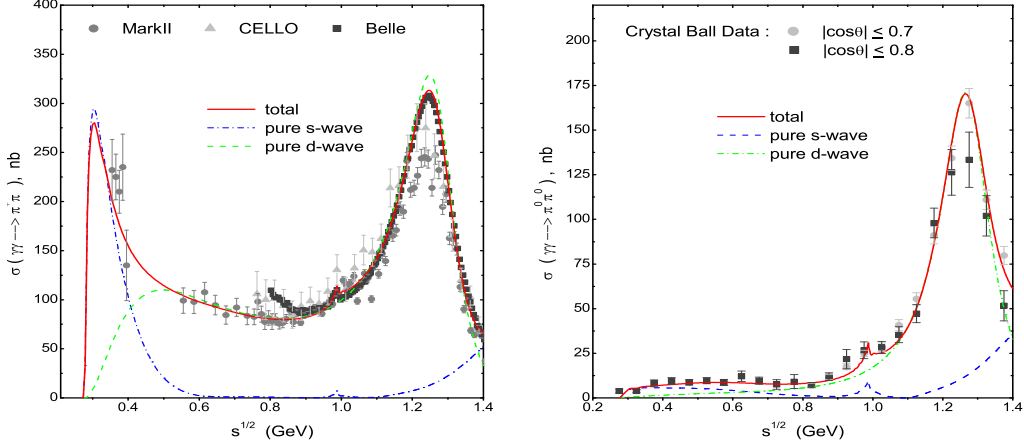


Figure 4: The coupled channel fit to the $\gamma\gamma \rightarrow \pi^+\pi^-, \pi^0\pi^0$ data. The data sets chosen are depicted in the text.

its residue are not quite stable, hence this number should be treated with care.

4. The σ width is smaller than most values given in the literature.

5.2 A refined analysis on the sigma coupling

We have noticed that the low energy physics related to the σ pole as described by the coupled channel T matrix is not very satisfactory. Because the lack of crossing symmetry, occurrence of spurious poles, and the distortion of the σ pole location. All these defects could affect a reliable extraction of the two photon coupling of the σ meson. We try to remedy these defects by refitting the low energy data using a single channel T matrix with all the nice properties such as analyticity, crossing symmetry, unitarity and with a reliable σ pole location, since there is no coupled channel T matrix with these properties available yet. The appropriate choice is the $\pi\pi$ scattering T matrix proposed in Ref. [19], which gives the σ pole location (The Eq. (21) of Ref. [19]):

$$M_\sigma = 457 \text{ MeV} , \quad \Gamma_\sigma = 551 \text{ MeV} , \quad (42)$$

and the residue:

$$g_{\sigma\pi\pi}^2 = (-0.20 - 0.13i) \text{ GeV}^2 , \quad (43)$$

$\chi^2_{d.o.f.}$	P_1	Pole-position (GeV)	$\Gamma(\sigma \rightarrow \gamma\gamma)$ (keV)
0.8	0.49	$0.457 - 0.276i$	2.08

Table 5: A single channel fit up to 0.8GeV data using T matrix of Ref. [19], with only one parameter P_1 .

to be compared with Eq. (40).⁴ Also the value in Eq. (43) is compatible with the result of Ref. [12, 36], $g_{\sigma\pi\pi}^2 = -0.25 - 0.06i\text{GeV}^2$.

We refit the $\gamma\gamma \rightarrow \pi^+\pi^-, \pi^0\pi^0$ data below 800MeV using that $T_{J=0}^{I=0}$ and $T_{J=0}^{I=2}$ matrices and keeping d -waves fixed by the coupled channel fit described in section 5. That means contributions from all other partial waves are treated as background. In this situation we fit with only single parameter P_1 , while keeping all other parameters fixed by the coupled channel fit. The result is given in table 5. We plot the fit curve in figure 5.

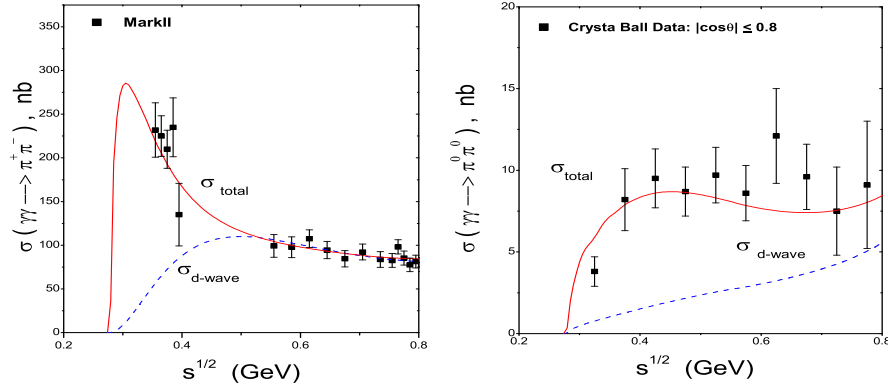


Figure 5: A fit up to 0.8GeV using single channel s -wave T matrices of Ref. [19], with one fit parameter P_1 . The $\pi^+\pi^-$ and $\pi^0\pi^0$ data are from Refs. [30] and [31], respectively. Dashed curve represents d -wave background, solid curve represents the total contributions, including the $I=0$ s -wave to be fitted.

5.3 A possible Breit–Wigner description to the $f_0(980)$ resonance

In this section we discuss the possibility that the two narrow width poles in the vicinity of $\bar{K}K$ threshold found in section 4 may be originated from a single Breit–Wigner parametrization.

⁴The $g_{\sigma\pi\pi}^2$ coupling differs by a factor 16π from that of Ref. [10] where the $g_{\sigma\pi\pi} \simeq 3\text{GeV}$. Ref. [10] also quoted the number extracted from Ref. [35] in two ways, corresponding to $|g_{\sigma\pi\pi}| = 3.4$ and 3.9GeV , respectively.

For the $\pi\pi, \bar{K}K$ coupled channel system, one can make use of conformal mapping technique [37] to map the four sheets s plane into the one sheet ω plane,

$$\omega = \frac{1}{\Delta}(p_1 + p_2) , \quad (44)$$

where $p_i = \frac{1}{2}\sqrt{s - 4m_i^2}$ denotes the i -th channel momentum, $\Delta = \sqrt{m_2^2 - m_1^2}$. The ω -plane is depicted in figure 6: In figure 6 $\omega = i, 1$ corresponds to $s = 4m_\pi^2$,

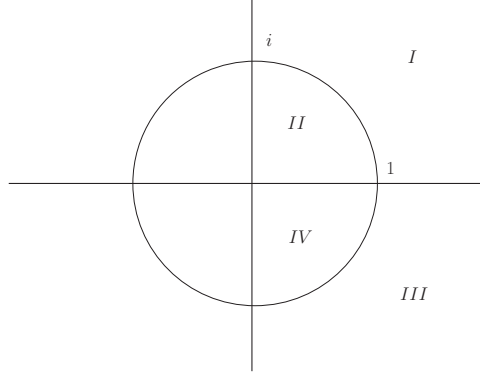


Figure 6: Conformal mapping and ω -plane.

$4m_K^2$, respectively. S matrix elements can be written as,

$$S_{11}(\omega) = \frac{d(-\frac{1}{\omega})}{d(\omega)}, \quad S_{22}(\omega) = \frac{d(\frac{1}{\omega})}{d(\omega)}, \quad \det S(\omega) = \frac{d(-\omega)}{d(\omega)} . \quad (45)$$

Function $d(\omega)$ contains no kinematical cut and $d(-\omega^*) = d^*(\omega)$, according to real analyticity. An S matrix pole corresponds to a zero of $d(\omega)$. We denote second sheet pole and third sheet pole by ω_2 and ω_3 , respectively and

$$\begin{aligned} \omega_2 &= r_2 \exp(i\phi_2) , & r_2 < 1 , & \phi_2 > 0 \\ \omega_3 &= r_3 \exp(i\phi_3) , & r_3 > 1 , & \phi_3 < 0 . \end{aligned} \quad (46)$$

The relations between r_i, ϕ_i and s -plane parameters $s_2 = (M_2 - \frac{i}{2}\Gamma_2)^2$, $s_3 = (M_3 - \frac{i}{2}\Gamma_3)^2$ are

$$\begin{aligned} M_i \Gamma_i &= \left(\frac{1}{r_i^2} - r_i^2\right) \Delta^2 \sin 2\phi_i , \\ M_i^2 - \Gamma_i^2/4 &= \left(\frac{1}{r_i^2} + r_i^2\right) \Delta^2 \cos 2\phi_i + 2(m_2^2 + m_1^2) . \end{aligned} \quad (47)$$

In such a two-pole case,

$$d(\omega) = d^{bg}(\omega) D(\omega) , \quad (48)$$

where

$$D(\omega) = \omega^{-2}(\omega - \omega_2)(\omega + \omega_2^*)(\omega - \omega_3)(\omega + \omega_3^*) \quad (49)$$

and then

$$S_{11} = \frac{D(-\omega^{-1})}{D(\omega)} \frac{d^{bg}(-\omega^{-1})}{d^{bg}(\omega)} = \frac{D(-\omega^{-1})}{D(\omega)} S^{bg}(\omega) . \quad (50)$$

One can prove, under some simplifications, that when $r_2 r_3 = 1$ the two pole description Eq. (50) is equivalent to the following coupled channel Breit–Wigner description [38],

$$\begin{aligned} S_{11}(s) &= \frac{s_0 - s - i\left(-\frac{p_1}{2m_K}\gamma_\pi + \frac{p_2}{2m_K}\gamma_k\right)}{s_0 - s - i\left(\frac{p_1}{2m_K}\gamma_\pi + \frac{p_2}{2m_K}\gamma_k\right)} \exp(2i\delta_{bg}) \\ &\simeq \frac{s_0 - s - i\left(-\rho_1 \frac{\gamma_\pi}{2} + \rho_2 \frac{\gamma_k}{2}\right)}{s_0 - s - i\left(\rho_1 \frac{\gamma_\pi}{2} + \rho_2 \frac{\gamma_k}{2}\right)} \exp(2i\delta_{bg}) , \end{aligned} \quad (51)$$

where

$$\begin{aligned} s_0 &= 4m_2^2 + \Delta^2 \left[\left(r_3 - \frac{1}{r_3}\right)^2 + 4 \sin \phi_2 \sin \phi_3 \right] , \\ \gamma_\pi &= 4m_2 \Delta \left(r_3 - \frac{1}{r_3}\right) (\sin \phi_2 - \sin \phi_3) , \\ \gamma_k &= 4m_2 \Delta \left(r_3 + \frac{1}{r_3}\right) (-\sin \phi_2 - \sin \phi_3) . \end{aligned} \quad (52)$$

The second equality in Eq. (51) hold approximately, because we limit ourselves in the energy region around $\bar{K}K$ threshold. Using the pole positions provided by table 2 and Eq. (47) we find the pole locations on the ω plane as following:

$$\begin{aligned} r_2 &= 0.82, \quad \sin \phi_2 = 0.12 , \\ r_3 &= 1.27, \quad \sin \phi_3 = -0.28 , \end{aligned} \quad (53)$$

from which one finds $r_2 r_3 = 1.04 \simeq 1$. This suggests that the table 2 does imply that $f_0^{II}(980)$ and $f_0^{III}(980)$ may come from the same Breit–Wigner resonance. The Breit–Wigner resonance parameters in Eq. (51) can be determined (taking $1/r_2$ as r_3) using Eq. (52),

$$s_0 = 0.982 \text{ GeV}^2, \quad \gamma_\pi = 0.146 \text{ GeV}^2, \quad \gamma_K = 0.304 \text{ GeV}^2 . \quad (54)$$

Moreover, using the information obtained from the T matrix fit on f_0^{II} coupling to $\pi\pi$ (see section 4),

$$(g_\pi^2)_{II} = (-0.071 - 0.011i) \text{ GeV}^2 , \quad (55)$$

and comparing it with Eq. (51) one can actually determine the background phase $\delta_{bg}(s)$ at $\sqrt{s} = 2m_K$ to be $\sim 91.8^\circ$,⁵ which is actually mainly contributed by the σ pole. [19] In this determination one make use of the fact that f_0 is

⁵This background phase has also been discussed in Ref. [39].

a narrow width resonance and hence one can assume $\delta_{bg}(s)$ calculated at the pole position is approximately real.

Table 4 further indicates that the f_0^{III} 's di-photon coupling is much larger than that of f_0^{II} : $|(g_\gamma^2)_{III}/(g_\gamma^2)_{II}| \simeq 3$. On the other side an analysis based on coupled channel Breit-Wigner description (Eq. (51)) and the two pole positions provided in table 4 gives the ratio to be ~ 1.5 . Though the two ratios are rather different, nevertheless they at least both predict $|(g_\gamma^2)_{III}| > |(g_\gamma^2)_{II}|$. Hence the two narrow width poles in the vicinity of $\bar{K}K$ threshold found in section 4 may still be considered as originated from a single Breit-Wigner parametrization, in support of an early suggestion of Ref. [28]. Of course much more efforts still need to be done to clarify such a issue.

6 Discussions and conclusions

A coupled channel dispersive analysis on the $\gamma\gamma \rightarrow \pi^+\pi^-, \pi^0\pi^0$ processes is made using a K matrix parametrization from Ref. [13], but refitted with the new K_{e4} data of Ref. [14]. The shape of different $\gamma\gamma \rightarrow \pi\pi$ partial wave cross-sections are similar to those given in Refs. [2, 9], though we have a smaller s wave contribution at $f_2(1270)$ peak comparing with Ref. [2]. Properties of two poles (one on sheet II, one on sheet III) found near $\bar{K}K$ threshold are investigated and it is found that the two poles may be explained as coming from a single Breit-Wigner parametrization. Our prediction on the two photon width of the second sheet $f_0(980)$ resonance as listed in table 4 is smaller comparing with most previous determinations found in the literature, but agrees with the solution B of Ref. [2].

A refined analysis on the di-photon coupling of $f_0(600)$ is made, using the single channel T -matrix (the PKU) parametrization established in Ref. [19, 40]. The PKU parametrization maintains the nice property such as unitarity, analyticity and (numerically) crossing symmetry. Our result in table 5 gives $\Gamma(\sigma \rightarrow 2\gamma) \simeq 2.1\text{keV}$, which is compatible with the result of Ref. [10], though in latter the investigation only is only confined in the energy region below 0.8GeV and the d -wave contribution is not considered.

However, by comparing table 4 and 5, we find that the di-photon coupling of the σ pole may not be very stable. Nevertheless one may argue, based on the analysis made in this paper, that the coupling ought to be significantly smaller than the estimate based on a simple $(\bar{u}u + \bar{d}d)/\sqrt{2}$ assignment. We borrow from Ref. [48] table 6 on radiative width of scalars in different modelings of their composition, adding the result from Ref. [43]. Clearly one reads from table 6 that a scalar with di-photon decay width significantly smaller than 4keV cannot be of a simple $\bar{q}q$ nature.⁶ It is argued in Refs. [50, 51] that the $f_0(600)$ is the chiral partner of the pseudo-goldstone boson, or the σ meson responsible for spontaneous chiral symmetry breaking. In this picture one expects the $f_0(600)$ meson can not be described simply by a pure $\bar{q}q$ or a

⁶See however Ref. [49].

composition	prediction	author(s)
$(\bar{u}u + \bar{d}d)/\sqrt{2}$	4.0	Babcock and Rosner [41]
$\bar{s}s$	0.2	Barnes [42]
gg	$0.2 \sim 0.6$	Narison [43]
$[ns][ns]$	0.27	Achasov <i>et al</i> [44]
$\bar{K}K$	0.6	Barnes[45]
	0.22	Hanhart <i>et al</i> [46]

Table 6: Summary of two photon decay width of scalars calculated in different models.

pure $\bar{q}^2 q^2$ picture, rather it is a mixture of many components of Fock state expansion, possibly includes a sizable glue content as well. [12, 36] It is nature then to expect that this property is reflected by its two photon coupling as suggested by the estimation made in this paper.

7 Acknowledgement

We would like to thank Stephan Narison for helpful discussions. Especially we are in debt to Zhi-Hui Guo for his very valuable help in estimating the vector meson exchange contributions. This work is supported in part by National Nature Science Foundation of China under Contract Nos. 10875001, 10721063, 10647113 and 10705009.

References

- [1] T. Mori *et al.* (Belle Collaboration), Phys. Rev. **D75**(2007)051101.
- [2] M. R. Pennington, T. Mori, S. Uehara, Y. Watanabe, Eur. Phys. J.**C56**(2008)1.
- [3] M. R. Pennington, invited talk at YKIS Seminar on *New Frontiers in QCD: Exotic Hadrons and Hadronic Matter*, Kyoto, Japan, 20 Nov - 8 Dec 2006. Prog. Theor. Phys. Suppl. **168**(2007)143.
- [4] D. Morgan, M. R. Pennington, Z. Phys. **C48**(1990)623; D. Morgan, M. R. Pennington, Z. Phys. **C37**(1988)431.
- [5] O. Babelon et al., Nucl. Phys. **B113**(1976)445; O. Babelon et al., Nucl. Phys. **B114**(1976)252.
- [6] G. Mennessier, Z. Phys. **C16**(1983)241.
- [7] A. V. Anisovich, V. V. Anisovich, Phys. Lett. **B467**(1999)289.

- [8] L. V. Fil'kov, V. L. Kashevarov, Phys. Rev. **C72**(2005)035211.
- [9] N. N. Achasov, G. N. Shestakov, arXiv:0712.0885 [hep-ph].
- [10] J. A. Oller, L. Roca, C. Schat, Phys. Lett. **B659**(2008)201.
- [11] J. Bernabeu, J. Prades, Phys. Rev. Lett. **100**(2008)241804.
- [12] G. Mennessier, S. Narison, W. Ochs, Phys. Lett. **B665**(2008)205.
- [13] K. L. Au, D. Morgan and M. R. Pennington, Phys. Rev. **D35**(1987)1633.
- [14] S. Pislak *et al.*, Phys. Rev. **D67**(2003)072004.
- [15] J. R. Batley et al (The NA48/2 Collaboration), Euro. Phys. J. **C54**(2008)411.
- [16] F. E. Low Phys. Rev. **96**(1954)1428; M. Gell-Mann, M. L. Goldberger, Phys. Rev. **96**(1954)1433; H. D. I. Abarbanel, M. L. Goldberger, Phys. Rev. **165**(1968)1594.
- [17] J. F. Donoghue and Barry R. Holstein, Phys. Rev. **D48**(1993)137; D. Morgan and M. R. Pennington, Phys. Lett. **B272**(1991)134
- [18] J. F. Donoghue, J. Gasser, H. Leutwyler, Nucl. Phys. **B343**(1990)341.
- [19] Z. Y. Zhou *et al.*, JHEP 0502(2005)043.
- [20] J. J. Wang, Z. Y. Zhou, H. Q. Zheng, JHEP **0512**(2005)019.
- [21] W. Ochs, Ph.D. thesis, Munich Univ., 1974.
- [22] D. H. Cohen *et al.*, Phys. Rev. **D22**(1980)2595.
- [23] A. Etkin *et al.*, Phys. Rev. **D25**(1982)1786 .
- [24] A. D. Martin, E. N. Ozmutlu, Nucl. Phys. B158(1979)520.
- [25] G. Costa *et al.*, Nucl. Phys. **B175**(1980)402.
- [26] V. A. Polychronakos *et al.*, Phys. Rev. **D19**(1979)1317.
- [27] M. P. Locher, V. E. Markushin, H. Q. Zheng, Eur. Phys. J. **C4**(1998)317.
- [28] D. Morgan, Nucl. Phys. **A543**(1992)632.
- [29] H. J. Behrend *et al.* (CELLO Collaboration), Z. Phys. **C56**(1992)381.
- [30] J. Boyer *et al.* (Mark-II Collaboration), Phys. Rev. **D42**(1990)1350.
- [31] H. Marsiske *et al.*(Crystal Ball Collaboration) Phys. Rev. **D41**(1990)3324.

- [32] J. K. Bienlein *et al*, *IX International Workshop on Photon-Photon Collisions*, San. Diego, 1992, ed. D. Caldwell and H. P. Parr (World Scientific, 1992) p.241.
- [33] F. E. Close, Z. P. Li and T. Barnes, Phys. Rev. **D43**(1991)2161.
- [34] M. Boglione, M. R. Pennington, Eur. Phys. J. **C9**(1999)11.
- [35] I. Caprini, G. Colangelo, H. Leutwyler, Phys. Rev. Lett. 96, 132001 (2006).
- [36] R. Kaminski G. Mennesier, S. Narison, to appear.
- [37] M. Kato, Ann. Phys.**31**(1965)130.
- [38] Y. Fujii, M. Kato, Nuovo Cimento **13A**(1973)311.
- [39] B. S. Zou, D. Bugg, Phys. Rev. **D48**(1993)3948.
- [40] Z. Y. Zhou, H. Q. Zheng, Nucl. Phys.**A775**(2006)212; H. Q. Zheng et al., Nucl. Phys. **A733**(2004)235;
- [41] J. Babcock, J. L. Rosner, Phys. Rev. **D14**(1976)1286.
- [42] T. Barnes, Phys. Lett. **B165**(1985)434.
- [43] S. Narison, Phys. Rev. **D73**(2006)114024; S. Narison, G. Veneziano, Int. J. Mod. Phys. **A4**(1989)2751; S. Narison, Nucl. Phys. **B509**(1998)312.
- [44] N. N. Achasov *et al.*, Z. Phys. **C16**(1982)55.
- [45] T. Barnes, Proc. *IXth Int. Workshop on Photon-Photon Collisions* (San Diego, 1992), ed. D. Caldwell and H. P. Paar(World Scientific, 1992.), p.263
- [46] C. Hanhart, Yu. S. Kalashnikova, A. E. Kudryavtsev, A. V. Nefediev, Phys. Rev. **D75**(2007)074015.
- [47] C. Amsler et al. (Particle Data Group), Phys. Lett. **B667**(2008)1.
- [48] M. R. Pennington, Mod. Phys. Lett. **A22**(2007)1439.
- [49] F. Giacosa, T. Gutsche, V. Lyubovitskij, Phys. Rev. **D77**(2008)034007.
- [50] H. Q. Zheng, Plenary talk given at *Workshop on Chiral Symmetry in Hadron and Nuclear Physics: Chiral07*, Osaka, Japan, 13-16 Nov 2007; Mod. Phys. Lett. **A23**(2008)2218.
- [51] Z. H. Guo, L. Y. Xiao, H. Q. Zheng, Int. J. Mod. Phys. **A22**(2007)4603; M. X. Su, L. Y. Xiao, H. Q. Zheng, Nucl. Phys. **A792**(2007)288.
- [52] J. Gasser, S. Bellucci, M. E. Sainio, Nucl. Phys. **B423**(1994)80.

- [53] M. Suzuki, Phys. Rev. **D47**(1993)1252.
 [54] H. Y. Cheng, Phys. Rev. **D67**(2003)094007.
 [55] Z. H. Guo, Phys. Rev. **D 78**(2008)033004.

8 Appendix

In this section we describe the method how we calculate various vector meson and axial vector meson exchange contributions to the Born term amplitude. We use Proca field to describe spin 1 fields. For the 1^{--} vector meson, the interaction lagrangian is

$$\mathcal{L}_{kin} = -\frac{1}{4} < V_{\mu\nu} V^{\mu\nu} - 2M_V^2 V^\mu V_\mu >. \quad (56)$$

Proca field is also suitable to describe the two types of axial vector meson contributions: $\overline{A}_\mu (J^{PC} = 1^{+-})$ and $\overline{B}_\mu (J^{PC} = 1^{+-})$.

For $\pi\pi\gamma$ vertices, the lowest order χPT amplitudes are calculable using the following interaction lagrangian: [52]

$$\begin{aligned} \mathcal{L}_2^{\chi PT} &= \frac{F^2}{4} < u^\mu u_\mu >, \\ \mathcal{L}_{int}(V) &= eC_V \varepsilon_{\mu\nu\rho\sigma} F^{\mu\nu} < V_\rho \{Q, u^\sigma\} >, \\ \mathcal{L}_{int}(\overline{B}) &= eC_B F^{\mu\nu} < \overline{B}_\mu \{Q, u^\nu\} >, \\ \mathcal{L}_{int}(\overline{A}) &= eC_A F^{\mu\nu} < \overline{A}_\mu [Q, u^\nu] >, \end{aligned} \quad (57)$$

where

$$\begin{aligned} V_\mu &= \begin{pmatrix} \frac{\rho_0}{\sqrt{2}} + \frac{\omega}{\sqrt{2}} & \rho^+ & K^{*+} \\ \rho^- & -\frac{\rho_0}{\sqrt{2}} + \frac{\omega}{\sqrt{2}} & K^{*0} \\ K^{*-} & K^{\overline{*}0} & -\phi \end{pmatrix}_\mu, \\ \overline{A}_\mu &= \begin{pmatrix} \frac{a_1^0}{\sqrt{2}} + \frac{f_1(1285)}{\sqrt{2}} & a_1^+ & K_{1A}^+ \\ a_1^- & -\frac{a_1^0}{\sqrt{2}} + \frac{f_1(1285)}{\sqrt{2}} & K_{1A}^0 \\ K_{1A}^- & K_{1A}^{\overline{0}} & f_1(1420) \end{pmatrix}_\mu, \\ \overline{B}_\mu &= \begin{pmatrix} \frac{b_1^0}{\sqrt{2}} + \frac{h_1(1170)}{\sqrt{2}} & b_1^+ & K_{1B}^+ \\ b_1^- & -\frac{b_1^0}{\sqrt{2}} + \frac{h_1(1170)}{\sqrt{2}} & K_{1B}^0 \\ K_{1B}^- & K_{1B}^{\overline{0}} & h_1(1380) \end{pmatrix}_\mu. \end{aligned} \quad (58)$$

The K_{1A} and K_{1B} mesons are mixed states,

$$\begin{aligned} K_{1A} &= \sin \theta K_1(1270) + \cos \theta K_1(1400), \\ K_{1B} &= -\sin \theta K_1(1400) + \cos \theta K_1(1270). \end{aligned} \quad (59)$$

The mixing angle $|\theta| = 37^\circ$ or 58° [53, 54, 55]. Comparing with Ref. [52], we also introduced $\overline{A}_\mu(1^{++})$ exchanges here except the $1^{--}, 1^{+-}$ contributions. Coefficients C_V, C_A, C_B are determined through $\rho(770) \rightarrow \pi\gamma$, $a_1(1260) \rightarrow \pi\gamma$ and $b_1(1235) \rightarrow \pi\gamma$ processes.

Invariant amplitudes A, B are obtainable using the above interaction lagrangian:

• $\gamma\gamma \rightarrow \pi^0\pi^0$: $\rho_0, \omega, b_1^0, h_1(1170)$ contributes here.

$$\begin{aligned}
A_{N,\rho}^t &= \frac{C_V^2}{9F^2} \frac{s - 4t - 4m_\pi^2}{M_\rho^2 - t}, \\
B_{N,\rho}^t &= \frac{C_V^2}{18F^2} \frac{1}{M_\rho^2 - t}, \\
A_{N,\omega}^t &= \frac{C_V^2}{F^2} \frac{s - 4t - 4m_\pi^2}{M_\omega^2 - t} = 9A_{N,\rho}^t(M_\rho \rightarrow M_\omega), \\
B_{N,\omega}^t &= \frac{C_V^2}{2F^2} \frac{1}{M_\omega^2 - t} = 9B_{N,\rho}^t(M_\rho \rightarrow M_\omega), \\
A_{N,b_1}^t &= \frac{C_B^2}{36F^2} \frac{s + 4t - 4m_\pi^2}{M_{b_1}^2 - t}, \\
B_{N,b_1}^t &= \frac{C_B^2}{72F^2} \frac{1}{M_{b_1}^2 - t}, \\
A_{N,h_1}^t &= \frac{C_B^2}{4F^2} \frac{s + 4t - 4m_\pi^2}{M_{b_1}^2 - t} = 9A_{N,b_1}^t(M_{b_1} \rightarrow M_{h_1(1170)}), \\
B_{N,h_1}^t &= \frac{C_B^2}{8F^2} \frac{1}{M_{b_1}^2 - t} = 9B_{N,b_1}^t(M_{b_1} \rightarrow M_{h_1(1170)}), \tag{60}
\end{aligned}$$

To get u channel contributions we only need to replace t by u in above expressions, i.e. $A_{N,i}^u = A_{N,i}^t(t \rightarrow u)$, $B_{N,i}^u = B_{N,i}^t(t \rightarrow u)$

• $\gamma\gamma \rightarrow \pi^+\pi^-$: π, ρ, b_1, a_1 contribute here.

$$\begin{aligned}
A_{C,\pi}^{Contact} &= \frac{4}{s}, \\
B_{C,\pi}^{Contact} &= 0, \\
A_{C,\pi}^t &= \frac{(2t + s - 2m_\pi^2)^2}{s^2} \frac{1}{(m_\pi^2 - t)}, \\
B_{C,\pi}^t &= \frac{1}{m_\pi^2 - t}, \\
A_{C,\rho}^t &= \frac{C_V^2}{9F^2} \frac{s - 4t - 4m_\pi^2}{M_\rho^2 - t} = A_{N,\rho}^t, \\
B_{C,\rho}^t &= \frac{C_V^2}{18F^2} \frac{1}{M_\rho^2 - t} = B_{N,\rho}^t,
\end{aligned}$$

$$\begin{aligned}
A_{C,b_1}^t &= \frac{C_B^2}{36F^2} \frac{s+4t-4m_\pi^2}{M_{b_1}^2-t} = A_{N,b_1}^t, \\
B_{C,b_1}^t &= \frac{C_B^2}{72F^2} \frac{1}{M_{b_1}^2-t} = B_{N,b_1}^t, \\
A_{C,a_1}^t &= -\frac{C_A^2}{4F^2} \frac{s+4t-4m_\pi^2}{M_{a_1}^2-t} = -9A_{N,b_1}^t(C_B \rightarrow C_A, M_{b_1} \rightarrow M_{a_1}), \\
B_{C,a_1}^t &= -\frac{C_A^2}{8F^2} \frac{1}{M_{a_1}^2-t} = -9B_{N,b_1}^t(C_B \rightarrow C_A, M_{b_1} \rightarrow M_{a_1}), \quad (61)
\end{aligned}$$

To get u channel contribution we only need to replace t by u in above expressions, i.e. $A_{C,i}^u = A_{C,i}^t(t \rightarrow u)$, $B_{C,i}^u = B_{C,i}^t(t \rightarrow u)$

• $\gamma\gamma \rightarrow K^+K^- : K, K^*, K_{1B}, K_{1A}$ contribute.

$$\begin{aligned}
A_{C,K}^{Contact} &= \frac{4}{s}, \\
B_{C,K}^{Contact} &= 0, \\
A_{C,K}^t &= \frac{(2t+s-2m_K^2)^2}{s^2} \frac{1}{(m_K^2-t)} = A_{C,\pi}^t(m_\pi \rightarrow m_K), \\
B_{C,K}^t &= \frac{1}{m_K^2-t} = B_{C,\pi}^t(m_\pi \rightarrow m_K), \\
A_{C,K^*}^t &= \frac{C_V^2}{9F_K^2} \frac{s-4t-4m_K^2}{M_{K^*}^2-t} = A_{N,\rho}^t(m_\pi \rightarrow m_K, M_\rho \rightarrow M_{K^*}, F \rightarrow F_K), \\
B_{C,K^*}^t &= \frac{C_V^2}{18F_K^2} \frac{1}{M_{K^*}^2-t} = B_{N,\rho}^t(m_\pi \rightarrow m_K, M_\rho \rightarrow M_{K^*}, F \rightarrow F_K), \\
A_{C,K_{1B}}^t &= \frac{C_B^2}{36F_K^2} \frac{s+4t-4m_K^2}{M_{K_{1B}}^2-t} = A_{N,b_1}^t(m_\pi \rightarrow m_K, M_{b_1} \rightarrow M_{K_{1B}}, F \rightarrow F_K), \\
B_{C,K_{1B}}^t &= \frac{C_B^2}{72F_K^2} \frac{1}{M_{K_{1B}}^2-t} = B_{N,b_1}^t(m_\pi \rightarrow m_K, M_{b_1} \rightarrow M_{K_{1B}}, F \rightarrow F_K), \\
A_{C,K_{1A}}^t &= -\frac{C_A^2}{4F_K^2} \frac{s+4t-4m_K^2}{M_{K_{1A}}^2-t} = -9A_{N,b_1}^t(C_B \rightarrow C_A, M_{b_1} \rightarrow M_{K_{1A}}, m_\pi \rightarrow m_K, F \rightarrow F_K), \\
B_{C,K_{1A}}^t &= -\frac{C_A^2}{8F_K^2} \frac{1}{M_{K_{1A}}^2-t} = -9B_{N,b_1}^t(C_B \rightarrow C_A, M_{b_1} \rightarrow M_{K_{1A}}, m_\pi \rightarrow m_K, F \rightarrow F_K). \quad (62)
\end{aligned}$$

To get u channel contributions we only need to replace t by u in above expressions, i.e. $A_{C,i}^u = A_{C,i}^t(t \rightarrow u)$, $B_{C,i}^u = B_{C,i}^t(t \rightarrow u)$

• $\gamma\gamma \rightarrow K^0\overline{K}^0 : K^*, K_{1B}$ contribute.

$$\begin{aligned}
A_{N,K^*}^t &= \frac{4C_V^2}{9F_K^2} \frac{s-4t-4m_K^2}{M_{K^*}^2-t} = 4A_{N,\rho}^t(m_\pi \rightarrow m_K, M_\rho \rightarrow M_{K^*}, F \rightarrow F_K), \\
B_{N,K^*}^t &= \frac{C_V^2}{18F_K^2} \frac{1}{M_{K^*}^2-t} = 4B_{N,\rho}^t(m_\pi \rightarrow m_K, M_\rho \rightarrow M_{K^*}, F \rightarrow F_K),
\end{aligned}$$

$$\begin{aligned}
A_{N,K_{1B}}^t &= \frac{C_B^2}{9F_K^2} \frac{s + 4t - 4m_K^2}{M_{K_{1B}}^2 - t} = 4A_{N,b_1}^t(m_{\pi \rightarrow m_K}, M_{b_1} \rightarrow M_{K_{1B}}, F \rightarrow F_K), \\
B_{N,K_{1B}}^t &= \frac{C_B^2}{18F_K^2} \frac{1}{M_{K_{1B}}^2 - t} = 4B_{N,b_1}^t(m_{\pi \rightarrow m_K}, M_{b_1} \rightarrow M_{K_{1B}}, F \rightarrow F_K),
\end{aligned} \tag{63}$$

To get u channel contributions we only need to replace t by u in above expressions, i.e. $A_{C,i}^u = A_{C,i}^t(t \rightarrow u)$, $B_{C,i}^u = B_{C,i}^t(t \rightarrow u)$.

In above formulas, in a term $A_{N(C),i}^{t(u)}$, the subscript $N(C)$ denote neutral (charged) particle exchanges. Superscript i means resonance R_i contribution in such channel, $t(u)$ denotes $t(u)$ channel.

One can hence get helicity amplitudes H_{++}, H_{+-} for processes $\gamma\gamma \rightarrow \pi^+\pi^-$, $\gamma\gamma \rightarrow \pi^0\pi^0$, $\gamma\gamma \rightarrow K^+K^-$, $\gamma\gamma \rightarrow K^0\bar{K}^0$:

$$\begin{aligned}
H_{++} &= A + 2(4m_\pi^2 - s)B, \\
H_{+-} &= \frac{8(m_\pi^4 - tu)}{s}B.
\end{aligned} \tag{64}$$

For example, for the $\gamma\gamma \rightarrow \pi^+\pi^-$ process, the helicity amplitude read,

$$\begin{aligned}
H_{++} &= A_{C,\pi}^{Contact} + A_{C,\pi}^{t+u} + A_{C,\rho}^{t+u} + A_{C,b_1}^{t+u} + A_{C,a_1}^{t+u} \\
&\quad + 2(4m_\pi^2 - s)(B_{C,\pi}^{Contact} + B_{C,\pi}^{t+u} + B_{C,\rho}^{t+u} + B_{C,b_1}^{t+u} + B_{C,a_1}^{t+u}), \\
H_{+-} &= \frac{8(m_\pi^4 - tu)}{s}(B_{C,\pi}^{Contact} + B_{C,\pi}^{t+u} + B_{C,\rho}^{t+u} + B_{C,b_1}^{t+u} + B_{C,a_1}^{t+u}). \tag{65}
\end{aligned}$$

The amplitudes H_{++}, H_{+-} are expressed using Condon-Shortly convention. M_{++}, M_{+-} used in this paper are defined using non Condon-Shortly convention

$$M_{++} = \frac{e^2 s}{2} H_{++}, \quad M_{+-} = \frac{-e^2 s}{2} H_{+-}. \tag{66}$$

Finally we plot in figure 7 various Born term contributions in $\pi^+\pi^-$ and $\pi^0\pi^0$ channels.

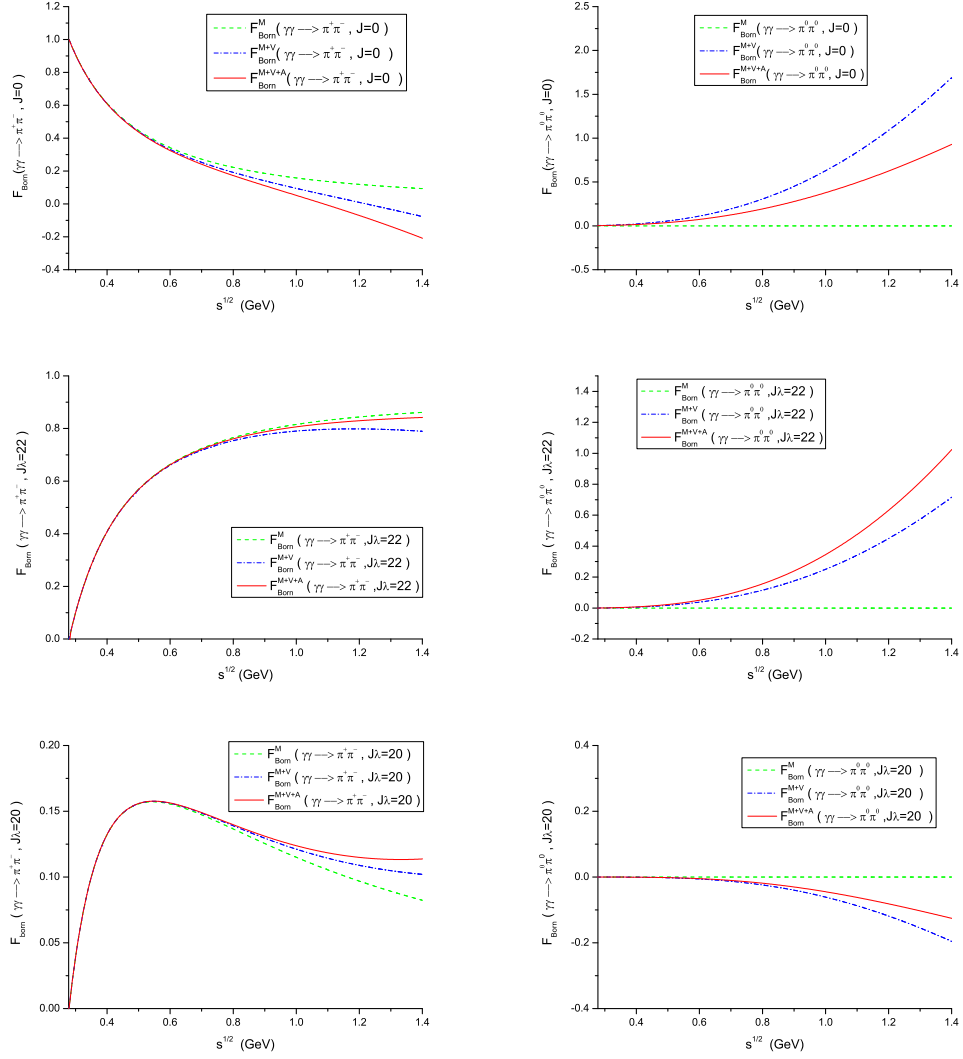


Figure 7: Born term contribution to $\pi^+\pi^-$ and $\pi^0\pi^0$ amplitudes.